Hydrogen Bonding in Helical Polypeptides from Molecular Dynamics Simulations and Amide Hydrogen Exchange Analysis: Alamethicin and Melittin in Methanol

Richard B. Sessions, Nick Gibbs, and Christopher E. Dempsey
Biochemistry Department and Centre for Molecular Recognition, Bristol University, School of Medical Sciences, Bristol BS8 1TD, United Kingdom

ABSTRACT Molecular dynamics simulations of ion channel peptides alamethicin and melittin, solvated in methanol at 27°C, were run with either regular α-helical starting structures (alamethicin, 1 ns; melittin 500 ps either with or without chloride counterions), or with the x-ray crystal coordinates of alamethicin as a starting structure (1 ns). The hydrogen bond patterns and stabilities were characterized by analysis of the dynamics trajectories with specified hydrogen bond angle and distance criteria, and were compared with hydrogen bond patterns and stabilities previously determined from high-resolution NMR structural analysis and amide hydrogen exchange measurements in methanol. The two alamethicin simulations rapidly converged to a persistent hydrogen bond pattern with a high level of 3_{10} hydrogen bonding involving the amide NH's of residues 3, 4, 9, 15, and 18. The 3_{10} hydrogen bonds stabilizing amide NH's of residues C-terminal to P2 and P14 were previously proposed to explain their high amide exchange stabilities. The absence, or low levels of 3_{10} hydrogen bonds at the N-terminus or for A15 NH, respectively, in the melittin simulations, is also consistent with interpretations from amide exchange analysis. Perturbation of helical hydrogen bonding in the residues before P14 (Aib10-P14, alamethicin; T11-P14, melittin) was characterized in both peptides by variable hydrogen bond patterns that included π and γ hydrogen bonds. The general agreement in hydrogen bond patterns determined in the simulations and from spectroscopic analysis indicates that with suitable conditions (including solvent composition and counterions where required), local hydrogen-bonded secondary structure in helical peptides may be predicted from dynamics simulations from α-helical starting structures. Each peptide, particularly alamethicin, underwent some large amplitude structural fluctuations in which several hydrogen bonds were cooperatively broken. The recovery of the persistent hydrogen bonding patterns after these fluctuations demonstrates the stability of intramolecular hydrogen-bonded secondary structure in methanol (consistent with spectroscopic observations), and is promising for simulations on extended timescales to characterize the nature of the backbone fluctuations that underlie amide exchange from isolated helical polypeptides.

INTRODUCTION

Alamethicin and melittin (see Fig. 1) are small amphipathic helical peptides that bind to and permeabilize membranes either through semi-specific voltage-gated ion channel activity or by nonspecific pore formation associated with disruption of membrane lipid organization. Despite spectroscopic evidence that the peptides are predominantly helical in membranes, membrane-bound high-resolution structures have not been determined and the most detailed structural information has come from x-ray crystallography and high-resolution NMR spectroscopy in methanol. However, even under conditions where intramolecular hydrogen-bonded secondary structure is stabilized, high-resolution NMR structures of these linear molecules are difficult to define due to the absence of long-range distance constraints required to establish helix bending, the poor definition of structural perturbations that result in local 3_{10}-, π-helix, or other nonregular structure, and the presence of dynamically disordered structure that is manifest in the absence of structure-defining NOE's. NMR analysis of alamethicin (Esposito et al., 1987; Yee and O'Neil, 1992) and melittin (Bazzo et al., 1988) established the overall α-helical conformations of these peptides in methanol, but detailed local hydrogen-bonded patterns, and the effects of the proline at residue 14 (Fig. 1) on helical structure and dynamics, have not been well defined. These properties are of interest in relation to the contribution of helix bending to ion channel gating (Fox and Richards, 1982; Sansom, 1993) and channel stabilities (Dempsey et al., 1991; Duclohier et al., 1992) in membrane-reconstituted forms of the peptides.

Amide exchange analysis of alamethicin (Dempsey, 1995) and melittin (Dempsey, 1988; 1992) in methanol demonstrated that the hydrogen bonding patterns and the effects of the P14 residue differ in the two peptides. Strong exchange stabilization of amides at the N-terminus (Aib 3 NH) and on the C-terminal side of P14 (V15 NH) indicate the presence of stable 3_{10} hydrogen bonds in alamethicin, whereas the absence of stable 3_{10} hydrogen bonds in melittin is apparent from the low exchange protection of the corresponding amide NH's of melittin (A4 NH and A15 NH; Fig. 1). The presence of proline 14 results in considerable loss of exchange stabilities for amides in a full turn of helix in melittin (residues 12–15 inclusive), whereas the

Received for publication 27 May 1997 and in final form 29 September 1997.

Address reprint requests to Dr. C. E. Dempsey, Biochemistry Department and Centre for Molecular Recognition, Bristol University, School of Medical Sciences, University Walk, Bristol BS8 1TD, UK. Tel.: (0)117 9287569; Fax: (0)117 9288274; E-mail: dempsey@bsa.bristol.ac.uk.

0006-3495/98/01/138/15 $2.00

corresponding amides of alamethicin are highly exchange-protected, presumably by intramolecular hydrogen bonds. In contrast to this evidence for stable hydrogen-bonded structure around P14 in alamethicin, spin label NMR relaxation enhancement in an alamethicin analog indicates significant helix bending induced by perturbation of helical structure around P14 (North et al., 1994). Structural disorder around G11-L12 is also apparent from analysis of amide temperature coefficients and ^{1}H, ^{15}N, and ^{13}C chemical shifts (Yee et al., 1995).

To determine the extent to which the differences in hydrogen bond structure and stabilities in alamethicin and melittin, inferred from amide exchange measurements, can be understood in terms of their intrinsic conformational and dynamic properties, we have carried out molecular dynamics simulations of the peptides solvated in methanol under periodic boundary conditions. Since NMR experiments indicate that the peptides adopt essentially α-helical structures in this solvent, we have used regular α-helical conformations as starting structures. An alamethicin simulation starting with the x-ray structure of Fox and Richards (1982) was also carried out, and melittin simulations were run either without or with charge-neutralizing chloride counterions. Here we present comparisons of the peptide hydrogen-bonded structures and stabilities determined from the dynamics trajectories with similar information from amide exchange analysis. Two levels of comparison are considered. First, since deviations from regular α-helical structure (for example, the presence of 3_{10} hydrogen bonds) arise largely from localized influences of side chains, these should be most accurately reproduced in simulations. The nature of larger-scale structural perturbations such as those responsible for loss of stable hydrogen bonding around P14 in melittin are difficult to characterize experimentally, but successful simulations should give some insight into the different effects of P14 on local hydrogen-bonded structure in the two peptides. Secondly, we consider the relationship between the hydrogen-bond breaking backbone fluctuations observed in the simulations and those that free hydrogen-bonded amides allowing exchange with solvent.

METHODS

General simulation conditions

Molecular mechanics calculations were carried using DISCOVER 2.95 (Biosym/MSI) with the CVFF force field (Dauber-Osguthorpe et al., 1988), and dynamics trajectories were analyzed using FOCUS (Sessions et al., 1989; Osguthorpe and Dauber-Osguthorpe, 1992). Minimum image periodic boundary conditions were used at constant volume. Nonbonded electrostatic and van der Waals forces were truncated to a 12 Å radius over a smoothing distance of 2 Å.

Solvent generation

The unit cell of the $-110°$ crystal structure of methanol (Tauer and Lipscomb, 1952) was replicated (5 × A, 4 × B, 7 × C) to generate 560 molecules. A semi-empirical orbital calculation on an isolated molecule (AMPAC using the AM1 Hamiltonian) followed by Mulliken analysis gave partial charges used for subsequent molecular mechanics calculations [H3 (0.00), C (0.10), O (-0.35), H (0.25)]. The orientations of the methanol molecules in the solvent box were randomized by performing 50 ps of molecular dynamics with a box size of 34 × 34 × 34 Å (the resulting density of methanol of 0.76 g cc^{-1} is close to the experimental value of 0.79 g cc^{-1} at 20°C). The dipole moment calculated from the partial charges (1.4 D) is somewhat smaller than the experimentally determined value (1.7 D; Weast, 1976).

Peptide construction and refinement

Right-handed α-helical polyalanine peptides were constructed using InsightII (Biosym/MSI) and "mutated" into the sequence of either alamethicin or melittin. Intramolecular van der Waals overlaps of 30% or more were removed by manual adjustment of the side chain torsion angles. Inevitable clashes between the proline residues and the surrounding sequences were ignored at this stage, since these could not be altered without disrupting α-helical conformations. Molecule A from the unit cell of the alamethicin x-ray structure (Fox and Richards, 1982; Brookhaven code 1AMT) was used as a starting structure for one simulation. The structures were centered in pseudo unit cells (alamethicin: 50 × 33 × 33 Å; melittin: 60 × 33 × 33 Å) with the helix axis oriented parallel to the longest side of the box. The cell dimensions were chosen to allow for at least 12 Å between any peptide atom and the peptide ghost of an adjacent cell. Each system was solvated in methanol such that all solvent molecules overlapping peptide atoms were removed, resulting in an even distribution of 675 molecules surrounding the alamethicin peptide and 794 around the melittin molecule. One melittin simulation was carried out at infinite dilution (i.e., no counterions were added to the melittin solvent box). The second melittin simulation contained six chloride counterions, introduced by replacement of a solvent molecule adjacent to each of the six positively charged groups of the peptide.

Energy minimization and molecular dynamics

First, the solvent alone was subjected to 1000 iterations of steepest descents minimization, keeping the peptide atoms fixed. This was followed by a further minimization in which solvent and peptide hydrogen atoms were unconstrained, but the peptide heavy atoms were tethered. This involved 1000 iterations of steepest descents, comprising 200-step intervals that used a consecutively decreasing harmonic restraining potential of 100, 50, 20, 10, and 5 kcal/Å imposed on the tethered atoms. Finally, the entire assembly of solvent and unconstrained peptide was minimized using 4000 iterations of conjugate gradient algorithms.

Simulations were carried out at 300 K with a constant temperature bath, using the Verlet integration method with a 1-fs time step. Structures were saved every 0.1 ps for analysis.

Methods of analysis

The atomic properties, hydrogen bond lengths and angles, backbone torsion angles and their averages and standard deviations, were extracted from the complete history files or from selected time periods of the trajectories. The hydrogen bond data was processed as described under Results to yield hydrogen bond lifetimes. Vicinal coupling constants ($^{3}J_{NHCH\alpha}$) were calculated from the simulations by determining the coupling constant from individual torsion angles using the Karplus equation (Pardi et al., 1984) at each time interval in the history file and averaging the value of J over the selected portion of the trajectory. Apparent J values were determined for Aib and Pro residues (lacking a CHα or NH proton) for comparison with apparent J values calculated from the crystal structure of alamethicin.

Amide hydrogen exchange data

Experimental pH-dependent hydrogen-deuterium exchange rates for alamethicin (Dempsey, 1995) and melittin (Dempsey, 1988; 1992) were con-

verted to exchange protection factors, apparent hydrogen bond lifetimes (Pastore et al., 1989; Dempsey et al., 1991), or apparent equilibrium constants for hydrogen bond-breaking backbone fluctuations underlying amide exchange [$K_{o(app)}$], according to Scheme 1 (see following section).

THEORY

Comparison of hydrogen bond lifetimes in simulated and experimental dynamics

The experimental parameter obtained from amide exchange analysis is an exchange protection factor (PF), the factor to which the exchange rate constant for a hydrogen-bonded amide is suppressed relative to exchange of a non-hydrogen-bonded amide in an unstructured polypeptide. Analysis of exchange data is made using the model of Linderstrom-Lang in which exchange occurs via transient opening of hydrogen bonds according to Scheme 1 (Hvidt and Neilsen, 1966; Englander and Kallenbach, 1984). In this model, exchange is suppressed from the hydrogen-bonded "closed" state (NHc) in equilibrium with an "open" state(s) (NHo) from which exchange occurs with characteristics of a free amide. In the majority of cases, and in the case of exchange from monomeric alamethicin and melittin in methanol (Dempsey, 1988; 1995), the fluctuations limiting exchange are in preequilibrium with the chemical exchange event (i.e., $k_2 \gg k_3$). In this situation neither of the rate constants, k_1 or k_2, is accessible, and the experimental exchange rate constant, k_{ex}, is equal to $(k_1/k_2)k_3$ or $K_o \cdot k_3$, where K_o is the equilibrium constant defining the backbone fluctuation opening a particular hydrogen bond. When corrections are made for sequence (Bai et al., 1993) and conformation-dependent (Dempsey, 1992; 1995) influences on k_3, the experimental exchange protection factor is equivalent to K_o (i.e., $PF = 1/K_o$).

$$NH_c \underset{k_2}{\overset{k_1}{\rightleftharpoons}} NH_o \overset{k_3}{\rightarrow} ND_o \qquad (1)$$

The relationship between experimental PF and K_o values is accurate within the model of Scheme 1 only if all potential influences on amide exchange properties other than hydrogen bonding are eliminated. While it is convenient to use K_o values in comparing experimental exchange data and simulated dynamics, there remains some uncertainty in correcting exchange data for sequence- and conformation-dependent influences on exchange, particularly in methanol. For example, the comparison of acid- and base-catalyzed exchange rates for alamethicin and melittin indicates that helix dipole effective charges can have significant effects on exchange kinetics. The protection factors used here have been corrected for helix dipole effects by averaging acid- and base-catalyzed protection factors that are approximately equally and oppositely affected by electrostatic effects like helix dipole charges. However, this method of determining protection factors introduces other uncertainties into their interpretation in terms of K_o values (see Dempsey, 1995). For this reason the K_o values used here are designated "apparent" K_o values ($K_{o(app)}$).

Analysis of the protein database indicates that a hydrogen bond is considered to be present if the bond length (H—O) is 2.5 Å or less, and the bond angle (N—H—O) is between 120 and 240° (180 ± 60°) (Baker and Hubbard, 1984). We used a slightly longer hydrogen bond distance criterion of 2.7 Å for comparing simulated and experimental data to accommodate thermal motions of 0.4–0.5 Å, which produce small transient excursions over the 2.5 Å limit that cannot be considered hydrogen-bond-breaking fluctuations (Gibbs et al., 1997; the effects of these thermal fluctuations can be seen in the hydrogen bond length trajectories of Fig. 9). Longer hydrogen bond length criteria were also used in comparison with amide exchange data in consideration that many of the small amplitude fluctuations observed in the simulation might not be sufficient to allow exchange to occur. The distance criterion was dominant in selection of hydrogen bonds, very few of which were eliminated through failure to satisfy the N—H—O bond angle criterion. The proportion of the dynamics trajectory in which hydrogen bond criteria are fulfilled for a given amide NH is denoted by "hydrogen bond percentage lifetime"; this parameter can be converted to an apparent equilibrium constant defining hydrogen bond opening and closing ($K_{o(app)}$) using the relationship: % hydrogen bond lifetime = $100/(1 + K_o)$ % (Pastore et al., 1989), allowing comparison with experimental $K_{o(app)}$ values calculated from amide exchange measurements. In such comparisons it should be borne in mind that the apparent K_o values from simulations are calculated from single trajectories obtained over a timescale that may or not be related to the timescale of backbone fluctuations limiting amide exchange (which is not known; see above). These points are considered further in the Discussion.

Starting conditions

The dynamics simulations were run with starting structures corresponding to regular α-helical conformations, and, for alamethicin, the crystal structure coordinates as a starting structure. The crystal structure coordinates for melittin were not used as a starting structure for dynamics calculation since melittin crystals comprise melittin tetramers crystallized from aqueous solution (Terwilliger and Eisenberg, 1982), and this structure is not representative of the methanolic monomeric state. Alamethicin crystals, on the other hand, were obtained by crystallization from methanol using acetonitrile (Fox and Richards, 1982). The NMR structures of the peptides in methanol are not well enough defined to be used as discrete starting structures. Regular α-helical starting structures were used for the following reasons. Hydrogen-bonded structure in alcoholic solution results from the preference of intramolecular hydrogen bonding over peptide-solvent hydrogen bonds. Maximization of helical hydrogen bonding is expected in methanol, and NMR data indicate that hydrogen-bonded conformations are

largely α-helical (rather than 3_{10}-helical) for each peptide (Esposito et al., 1987; Bazzo et al., 1988). Deviations from regular α-helical structure due to the intrinsic conformational preferences of the peptides (resulting, for example, from the P14 residue, the high Aib content of alamethicin, the amino acid sequences and end effects) are expected to be apparent in the simulations. Additionally, convergence in the structural properties starting from α-helical or crystal structure coordinates in the alamethicin simulations is expected if the intrinsic conformational properties of the peptide are correctly sampled. Melittin simulations were run at a nominal pH of 5 so that each of the 6 titratable amino acids (G1; K7, 21, 23; R22, 24) were protonated (overall charge = +6). The variant of alamethicin used in the amide exchange and simulation studies (A6,Q18 alamethicin; Fig. 1) is uncharged.

RESULTS

Melittin

The starting and final (500 ps) structures of melittin in the simulations in methanol from α-helix with and without counterions are shown in Fig. 2. The absence of counterions results in unfolding of the melittin helix, in particular the C-terminal segment where four positively charged side chains are located (-K21-R-K-R24-), but also the N-terminal helix (two positive charges; N-terminal amino, and K7). During the simulation the C-terminal helix unwinds sequentially from the C-terminus, and this is manifest by an upward drift in the root mean square deviation (RMSD) of Cα atoms (Fig. 3), and sequentially decreasing H bond lifetimes from residue 18 to the C-terminus when averaged over the full simulation (Fig. 4 *A*). Since the latter observation is incompatible with the experimentally determined stability of the helical conformation of melittin in methanol (Bazzo et al., 1988; Dempsey, 1988), this simulation is not described further.

Inclusion of counterions greatly stabilizes the melittin conformation with the retention of stable N- and C-terminal helical sections throughout the simulation (Figs. 2 and 4 *B*). Stable hydrogen bonding in the region around P14 is not maintained, and this results in a profile of log $K_{o(app)}$ values that is broadly similar to the profile determined from the experimental amide exchange data (Fig. 5). The main features are the destabilization of hydrogen bonds in a full helical turn (amide NH of residues 12–15 inclusive; Fig. 4 *B*) and the increased stability of the C-terminal helix relative to the N-terminal helix. The destabilization of helical hydrogen bonding at the C-terminus (helix fraying) observed in the exchange data is not so marked in the simulations.

Although detailed analysis of the counterion trajectories is not presented here, the counterions remained close to their charge partners throughout the simulation and did not exchange between the peptide charged groups. This is largely an effect of the low dielectric medium in which electrostatic interactions are enhanced, since counterions within simulations of charged polypeptides in water migrate among fixed charges [as found, for example, in a previous simulation of melittin characterizing peptide solvation (Kitao et al., 1993)]. The inclusion of explicit counterions in simulations of charged polypeptides has been shown elsewhere to be important in reproducing experimental properties (e.g., Kitson et al., 1993; Schiffer and VanGunsteren, 1996; Young et al., 1997), and the requirement for counterions in reproducing the high stability of the melittin C-terminal helix (Fig. 4) indicates their importance in simulations in lower dielectric media than water. Although the amide exchange data were obtained in buffer-free solution (Dempsey, 1988; 1992), NMR samples at 2–3 mM peptide concentration contained 12–18 mM (chloride) counterions (i.e., one counterion for each of the six fixed charges of the peptide). Counterion condensation in methanol similar to that observed in the simulations may contribute to the high stability of the highly positively charged C-terminal helix observed experimentally.

Hydrogen bond lifetimes calculated from amide exchange protection factors are greater than those calculated from simulated percentage lifetimes, so that there is a displacement of experimental (amide exchange) $K_{o(app)}$ values below the simulated values (Fig. 5). This results from different definitions of hydrogen bonds in the two methods (satisfying distance and angle H bond constraints in the simulations, and the suppression of amide exchange according to Scheme 1 in experiment). The simulated values can be made to approach the experimental values by relaxing the hydrogen bond criteria (Fig. 5); the significance of this is described in the Discussion.

While the C-terminal helix (residues 16–26) retained stable α-helical hydrogen bonding throughout the simulation, hydrogen-bonded structure in the N-terminal helix was less stable. Fluctuations among different hydrogen bond patterns, as well as sequential loss of helical hydrogen bonding, both contribute to this conformational heterogeneity, as shown in Fig. 6, which illustrates residue-specific percentages of 3_{10}-, α-, and π-helix hydrogen bonds during sequential 100-ps intervals of the simulation. Two essential similarities with the hydrogen bond patterns and stabilities determined from the amide exchange data are apparent. First, the stability of the C-terminal helix results from the retention of stable α-helical hydrogen bonding with little transition between α and 3_{10} hydrogen bonds except for the

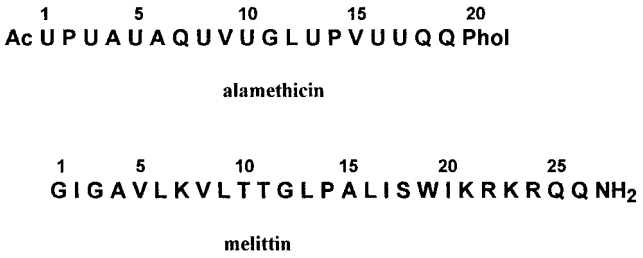

FIGURE 1 Amino acid sequences of melittin and the alamethicin variant used in this study. Phol is phenylalaninol; U is α-aminoisobutyric acid (Aib) (Sansom, 1993).

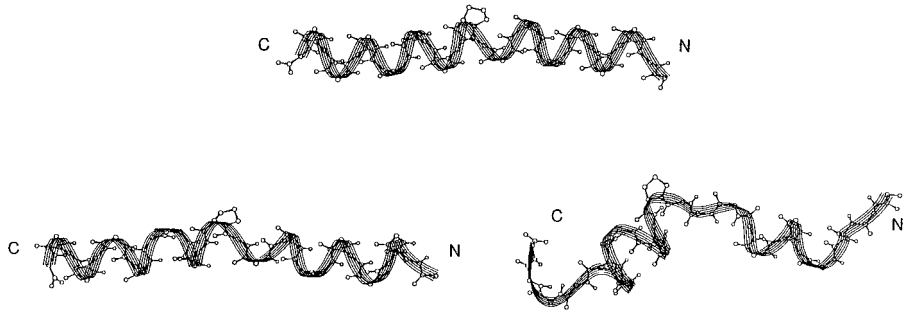

FIGURE 2 Starting (*top*) and final (*bottom*) structures of melittin before and after 500 ps molecular dynamics simulation from ideal α-helical structure in methanol run either with (*left*) or without (*right*) charge-neutralizing chloride counterions.

C-terminal residues (especially Q25 NH). The levels of π-helix hydrogen bonds was $<1\%$ for all residues C-terminal to P14. Secondly, the absence (A4 NH), or low levels (A15 NH), of 3_{10} hydrogen bonds for A4 and A15 NH is consistent with the low exchange stabilities of these residues observed in the amide exchange studies from which the absence of 3_{10} hydrogen bonding was inferred (Dempsey, 1988; Fig. 5).

The hydrogen bonding pattern for the N-terminal helix, while dominated by α-helical hydrogen bonding for residues 7–11, is variable at either end (Fig. 6). Sequential loss of stable hydrogen bonding for residues V5 and L6 occurs throughout the simulation. Loss of stable hydrogen bonding for residues G12 and L13, apparent at the end of the simulation, occurs with a high variation in hydrogen bonding of residues 11–13. The structure for these residues, initially mixed α- and 3_{10}-helical, is characterized by transitions between α- and π-helical hydrogen bonding from which stable α-helical hydrogen bonding for T11 NH is recovered after $\sim$300 ps of the simulation from a state in which the N-terminal helix has a high proportion of π-helix (Fig. 6). The disordered structure in residues 12–15 and the progressive loss of stable hydrogen bonding in the N-terminal residues are largely responsible for the drift of Cα RMSD to a value of $\sim$3 Å at the end of the simulation (Fig. 3).

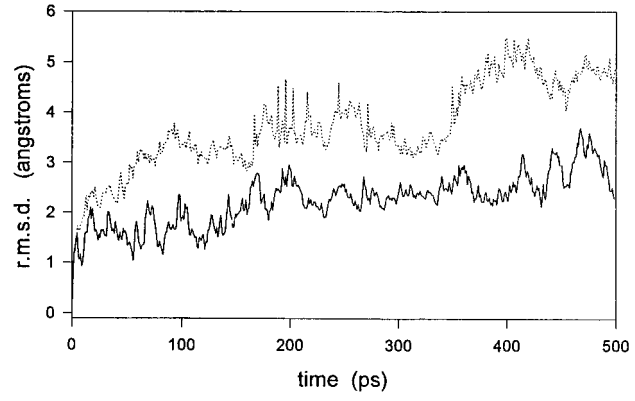

FIGURE 3 Root mean square deviation (RMSD), relative to α-helical starting structure coordinates, of Cα atoms of melittin during molecular dynamics simulation with (*solid line*), and without (*dotted line*) counterions.

As observed for G11 in the alamethicin simulations (Gibbs et al., 1997), the structure at G12 in melittin is characterized by a significant proportion of states in which the X-G peptide bond partially reverses. This peptide bond reversal is often associated with nonregular hydrogen bonds (G12NH-T10 carbonyl; inverse γ turn, and L13NH-V8 carbonyl; π-helix), as described for alamethicin (Gibbs et al., 1997). A representative example of this structure is shown in Fig. 7.

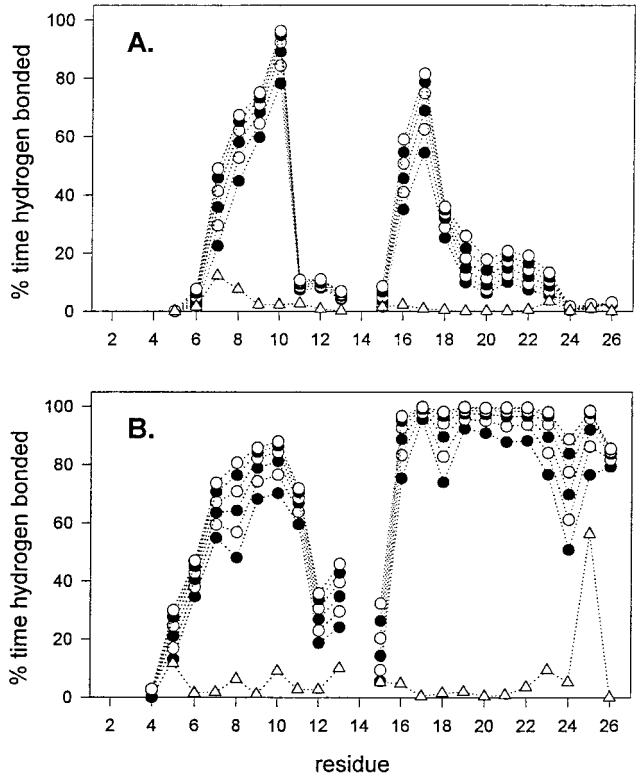

FIGURE 4 Residue-specific values for percentage hydrogen bond lifetimes during molecular dynamics simulation of melittin without (*A*) and with (*B*) counterions. Hydrogen bond lifetimes are the percentage of total trajectory in which the amide NH formed an intramolecular hydrogen bond with distance criteria (NH-OC) of 2.5 to 3.0 Å in 0.1-s steps (*lower filled circle* to *upper circle*). Open triangles define the contribution of 3_{10} hydrogen bonds to the hydrogen bond lifetimes with a 2.5 Å distance criterion. Dotted lines are drawn to guide the eye.

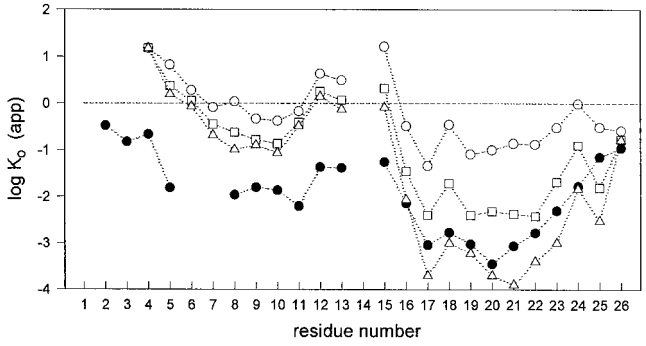

FIGURE 5 Comparison of log $K_{o(app)}$ values for melittin (see Scheme 1) calculated from amide hydrogen exchange protection factors in methanol (●), with values calculated from percentage hydrogen bond lifetimes from dynamics simulation with counterions using distance criteria of 2.5 (○), 2.7 (□), or 3.0 Å (△). Dotted lines are drawn to guide the eye.

Alamethicin

The starting and final structures from the alamethicin simulations run with either ideal α-helix or the x-ray crystal structures are shown in Fig. 8. Although the final structures in each case are bent due to disruption of regular helix around residues G11-U13, the bent structures are not representative of the full trajectories, which are better characterized by fluctuations between straight (helically hydrogen-bonded) and bent structures (Gibbs et al., 1997). In each simulation α-helical structure was generally maintained throughout, and the high levels of 3_{10} hydrogen bonding described below result from local deviations from α-helical structure that were established during the first few picoseconds of the simulations. Fig. 9 illustrates initial periods of hydrogen bond length trajectories for three of the amide NH's (V9, V15, and Q18), which form 3_{10} hydrogen bonds. These show rapid equilibration to dynamic states in which 3_{10} hydrogen bond constraints are satisfied relative to α-helical hydrogen bonds. Since the general hydrogen bond fluctuations were quite evenly distributed as reflected in the fluctuations, usually associated with helix bending, around a Cα RMSD near 2 Å (Fig. 10), hydrogen bond lifetimes and other descriptive parameters averaged over the full trajectories were similar to the parameters averaged over discrete periods. Figs. 11 and 12 illustrate residue-specific percentage hydrogen bond lifetimes from the α-helical simulation averaged over the full trajectory, and a comparison of $K_{o(app)}$ values from experimental amide exchange data (Dempsey, 1995) with corresponding values calculated from the simulations. Particularly prominent are the high exchange stabilities of V15 NH (C-terminal to P14) and of amides at the helix termini (e.g., U3 NH and the NH's of residues 18–19). The simulation starting from α-helical geometry shows better agreement with amide exchange stabilities than the simulation from the x-ray structure (not shown), although there is considerable convergence in the simulations as described below. Each simulation shows high stability of V15 NH hydrogen bonding and stable hydrogen bonding at the N- and C-termini apart from a loss of hydrogen bonding for the C-terminal Phol20 NH in the simulation from α-helix (Fig. 11).

The evolution of the hydrogen-bonding pattern in the alamethicin simulation from α-helical starting structure is shown in Fig. 13 as percentage hydrogen bond lifetimes averaged over 100-ps intervals. The high overall stability of intramolecular (generally helical) hydrogen bonding is apparent in the maintenance of high proportions of hydrogen bonding for all residues except Phol20 NH. Unlike melittin, in which stable hydrogen-bonded secondary structure is largely α-helical, the hydrogen bond pattern of alamethicin shows considerable 3_{10} helical structure even though the stable helical regions (residues 1–10 and 12–19) have an overall α-helical structure. Small local deviations (overtwisting) of α-helical structure results in a specific set of amide NH's forming 3_{10} hydrogen bonds (those of residues 3, 4, 9, 15, and 18). This hydrogen bond pattern is independent of the nature of the starting structure (regular α-helix or x-ray crystal structure; Figs. 13 and 14). The hydrogen bonding pattern is recovered after large amplitude backbone fluctuations involving breaking of several sequential hydrogen bonds such as those described in the Discussion. This can also be seen, for example, in the recovery of stable (α- and 3_{10}-) helical hydrogen bonding at the N-terminus after reversible fluctuations involving loss of hydrogen bonds for amides of residues 3–5 between 400 and 700 ps manifest by low percentage lifetimes during these periods of the trajectory (Fig. 13).

As in the melittin simulation, fluctuations in the structure comprising the residues before P14 result in variable hydrogen bond patterns. In each peptide large amounts of π-helical hydrogen bonding of residues 12 and 13 are observed as well as the reversal of the X-Gly peptide bonds with the formation of transiently stable inverse γ-turn structure (Gibbs et al., 1997). Unlike melittin, in which hydrogen-bonded structure in these residues is lost as the simulation progresses (Fig. 6), the hydrogen-bonded structure involving amide NH's of residues 11, 12, and 13, although variable, is persistent (Fig. 13).

DISCUSSION

Hydrogen-bonded structure in alamethicin and melittin in methanol

Significant stabilization of an amide to exchange with solvent in an isolated helical peptide indicates that the amide NH participates in an intramolecular hydrogen bond. Differences in exchange stabilization of backbone NH's in melittin (Dempsey, 1988; Fig. 5) and alamethicin (Dempsey, 1995; Fig. 12) therefore demonstrate differences in the hydrogen bond patterns and stabilities in the two peptides. In the first part of the discussion we describe interpretations of hydrogen-bonded structure from consideration of the amide exchange data and the dynamics simulations. In the second part we briefly consider the relationship between

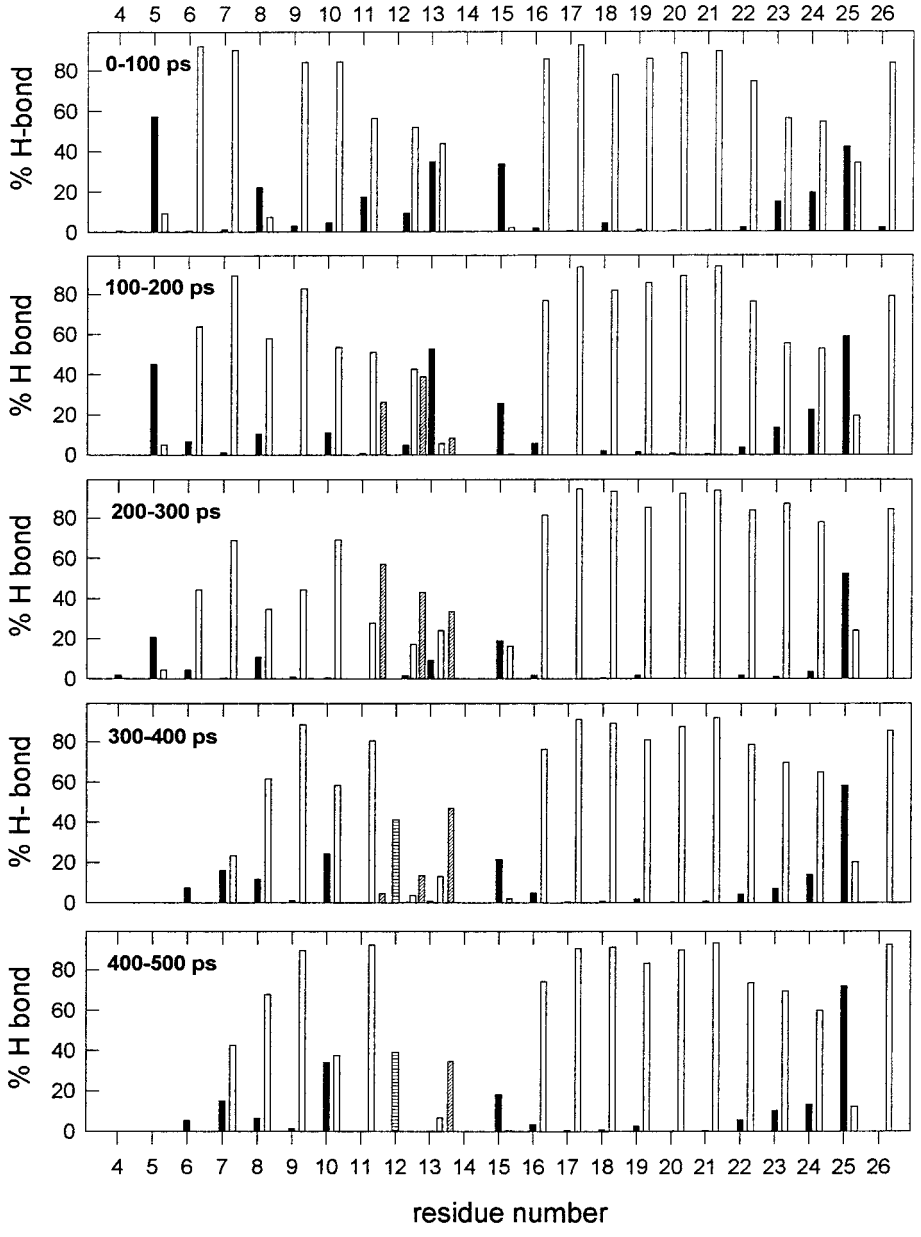

FIGURE 6 Percentage hydrogen bond lifetimes for amide NH's of melittin (3 Å criterion) averaged over 100-ps intervals of dynamics trajectories for the simulation with counterions. Hydrogen bond types are designated by: γ-turn (G12 NH; *horizontal hash*), 3_{10} helix (*filled bars*), α-helix (*open bars*), and π-helix (*diagonal hash*). Space is allocated to γ- and π-hydrogen bonds only for residues 11–13, since the occurrence of these hydrogen bond types is negligible in other residues.

hydrogen bond-breaking backbone fluctuations observed in the simulations and those that allow amide exchange.

Both alamethicin and melittin adopt largely α-helical conformations in methanol as indicated by observation of structurally diagnostic NOE's, particularly NH_i-$CH\alpha_{i-4}$ NOE's, which define α-helix over 3_{10} helix (Esposito et al., 1987; Bazzo et al., 1988; Yee and O'Neil, 1992; Yee et al., 1995). Detailed descriptions of local hydrogen-bonded secondary structure and the effects of the P14 residue on helix bending has been more difficult to define, especially in alamethicin, for which NOE structural information is lost by the absence of the α-carbon proton on Aib residues. Amide exchange protection factors (Dempsey, 1995) and amide temperature coefficients (Yee et al., 1995) indicate that the amides of residues Aib3 and V15 (on the C-terminal side of P2 and P14, respectively) are stabilized by 3_{10} hydrogen bonds, whereas the contribution of 3_{10} hydrogen bonding to stabilization of amides at the N-terminus, and of A15 NH (C-terminal to P14) is absent or small in melittin (Dempsey, 1988). The simulations are entirely consistent with these interpretations. A persistent 3_{10} hydrogen bond involving Aib3 NH and the N-terminal acetyl carbonyl group is maintained throughout both alamethicin simulations, despite large amplitude structural fluctuations in which this hydrogen bond breaks and reforms, resulting in low percentage hydrogen bond lifetimes during periods of the trajectories (e.g., 400–600 ps of the simulation from α-helical structure; Fig. 13). In contrast, 3_{10} hydrogen bonding never stabilizes A4 NH at the melittin N-terminus (Figs. 4 *B* and 6).

The major hydrogen-bonded structure found in both alamethicin simulations yields almost maximal elimination of

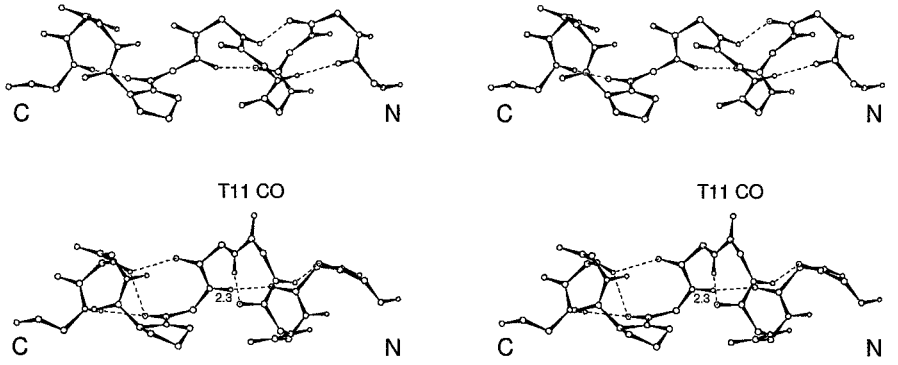

FIGURE 7 Stereo figure of structure near P14 in melittin extracted from dynamics simulation trajectories in methanol with counterions. Representative structures show either largely normal helix geometry (*upper figure*; after 125 ps of simulation), or a partially reversed T11-G12 peptide bond with inverse γ-turn and π-helix hydrogen bonds involving amide NH's of G12 and L13, respectively (*lower figure*; 328 ps).

exposed polar groups at the N-terminus. The acetyl group serves both to eliminate the N-terminal positive charge and to provide a 3_{10} carbonyl partner for Aib3 NH. P2 acts as a helix capping residue, additionally stabilizing the 3_{10} hydrogen-bonded structure. This suppression of exposed polar groups at the N-terminus contributes to the insertion of the alamethicin helix into membranes, a process which recent evidence suggests is favorable in the absence of a transmembrane potential (Barranger-Mathys and Cafiso, 1996). It may be predicted that the N-terminal sequence N-acetyl-X-Pro-X-X, where amino acids at positions X are nonpolar and helix-favoring, will generally promote membrane insertion of helical polypeptides.

Like proline 2 in alamethicin, proline 14 promotes 3_{10} helical hydrogen bonding (A15 NH-G12 carbonyl in melittin; V15 NH-L12 carbonyl in alamethicin). This property of proline in α-helix, noted previously (Piela et al., 1987; Fraternali, 1990; Yun et al., 1991) may be associated with the preference for peptide bonds of proline in α-helix to adopt conformations close to those of residue $i+2$ in a type III β-turn (ϕ $-60°$, ψ $-30°$, Rose et al., 1985); e.g., the torsion angles (average $\pm$ standard deviation) in the alamethicin simulations from x-ray and α-helical starting structures, respectively, are: Pro14: ϕ $-$ 67 $\pm$ 10°, ψ $-$ 26 $\pm$ 16°; Pro2: ϕ $-$ 58 $\pm$ 11°, ψ $-$ 35 $\pm$ 17°; Pro14: ϕ $-$ 66 $\pm$ 10°, ψ $-$ 28 $\pm$ 14°; Pro2: ϕ $-$ 62 $\pm$ 13°, ψ $-$ 22 $\pm$ 40°; and in the melittin simulation with counterions: Pro14: ϕ $-$ 55 $\pm$ 9°, ψ $-$ 41 $\pm$ 9°. A type III β-turn is essentially equivalent to a single turn of 3_{10} helix, with the 3_{10} hydrogen bond corresponding to the transannular hydrogen bond of the β-turn (Rose et al., 1985). This structure may be promoted by the preference for intramolecular hydrogen bonds in methanol. Whereas the V15 NH 3_{10} hydrogen bond is highly populated in alamethicin ($\sim$65% of both trajectories measured with a 2.7 Å criterion) it persists during $<$20% of the melittin trajectory (2.7 Å distance criterion). This results from the high conformational flexibility around G12 in melittin (see below) whose amide carbonyl is less easily constrained as a 3_{10} hydrogen bond acceptor than the L12 carbonyl of alamethicin. The much greater stability of this 3_{10} hydrogen bond in alamethicin compared with melittin is consistent with the greater exchange stability of V15NH of alamethicin (Fig. 12) compared with A15 NH of melittin (Fig. 5).

The high proportion of Aib in alamethicin contributes both to helix stability and to 3_{10} helical hydrogen bonding. The residue resists deviations from helical geometry, which is apparent in the low variation in phi and psi angles for Aib's during the dynamics trajectories (see Gibbs et al., 1997). Local structural relaxation occurred in the early sections of both alamethicin simulations to yield a persistent pattern in which the amides of residues 3, 4, 9, 15, and 18 are exclusively, or largely, stabilized in 3_{10} hydrogen bonds rather than α-helical hydrogen bonds (Figs. 11, 13, and 14). Only a small amount of 3_{10} hydrogen bonding is observed in melittin apart from some nonpersistent 3_{10} hydrogen

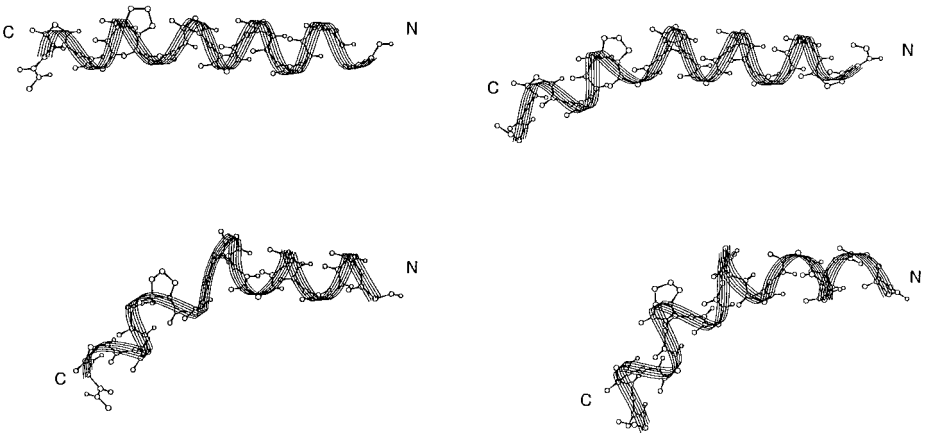

FIGURE 8 Starting (*top*) and final (*bottom*) structures of alamethicin after 1-ns simulation in methanol from ideal α-helix (*left*) or the x-ray crystal structure coordinates (*right*).

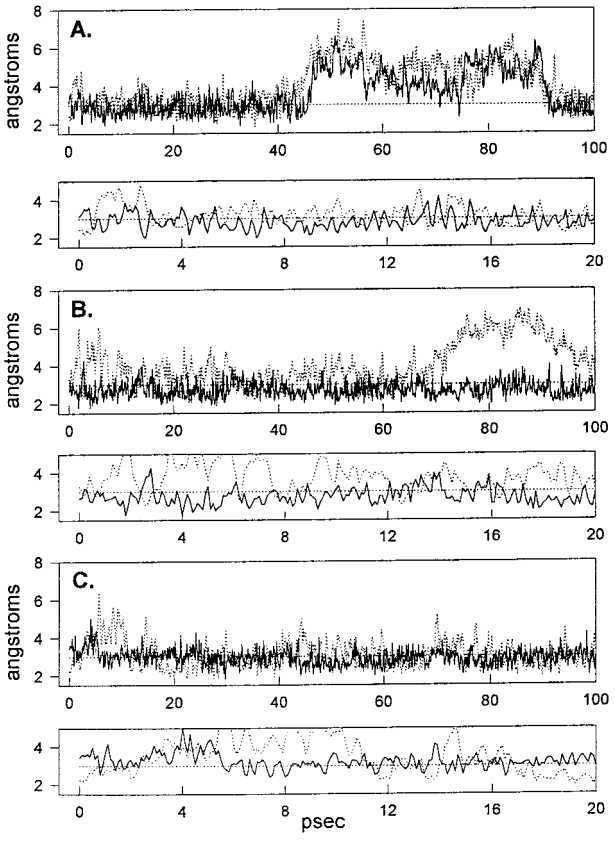

FIGURE 9 Initial periods of dynamics trajectories for three residues of alamethicin [V9 NH (*A*); V15 NH (*B*); Q18 NH (*C*)] which form 3_{10} hydrogen bonds during dynamics simulations in methanol. Evolution of NH to carbonyl oxygen distances for 3_{10} hydrogen bonds (*bold lines*) and α-helix hydrogen bonds (*broken lines*) are shown over the first 100 ps and expanded to show the first 20 ps in detail. The 3 Å distance is indicated by a horizontal dotted line.

bonds of V5 NH that occur during unfolding of the N-terminal residues, and R25 NH, which shows a high proportion of 3_{10} hydrogen bonding (Fig. 6). The high stability of α-helical secondary structure in the C-terminal helix of

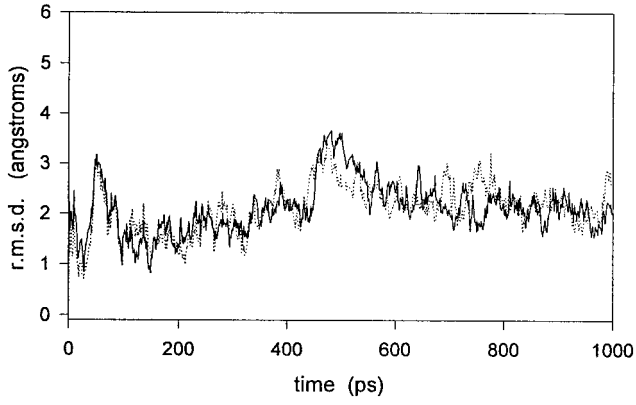

FIGURE 10 RMSD of Cα atom coordinates of alamethicin, relative to starting (regular α-helix) or to the x-ray crystal structure coordinates (Fox and Richards, 1982), during molecular dynamics simulation in methanol from an α-helical starting structure.

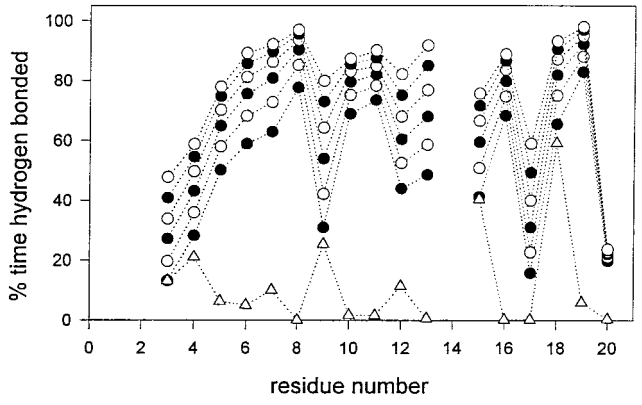

FIGURE 11 Residue-specific values for percentage hydrogen bond lifetimes during molecular dynamics simulation of alamethicin from α-helical starting structure. Symbols illustrate values for hydrogen bond distance constraints of 2.5–3.0 Å according to the legend to Fig. 4. The open triangles define the contribution of 3_{10} hydrogen bonds to the total hydrogen bond lifetimes with a 2.5 Å distance criterion.

melittin (Fig. 6) agrees with NMR measurements in which a near complete set of NH_i-$CH_{\alpha i-4}$ NOE's was observed for residues 16–24 (Bazzo et al., 1988).The greater stability of the melittin C-terminal helix compared to the N-terminal helix, which shows persistent hydrogen bonding only for amides of residues K7-T11 (Fig. 6), is similar to the conclusions from amide exchange analysis (Dempsey, 1988; Fig. 5).

Apart from Aib3 NH, the Aib residues themselves (Aib 5, 8, 10, 13, 16, and 17) show low levels of 3_{10} hydrogen bonding in alamethicin but induce high levels in the surrounding residues; generally, the Aib residues promote 3_{10} hydrogen bonds involving the NH of residue $i + 1$ or $i + 2$ (where Aib is residue i). In many structures the hydrogen bond carbonyl acceptor in a 3_{10} hydrogen bond is bifurcated, participating additionally in an α-helical hydrogen bond. Previous modeling studies have indicated that steric

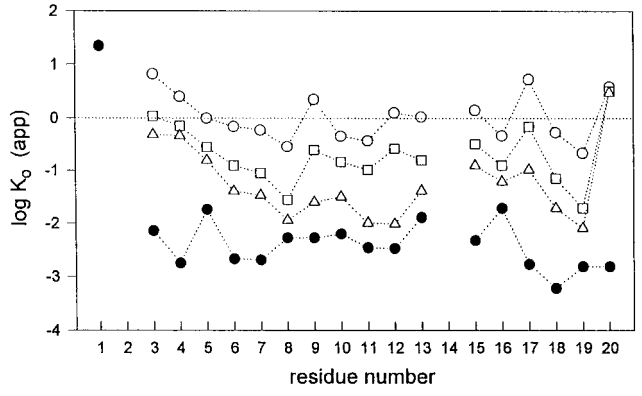

FIGURE 12 Comparison of log $K_{o(app)}$ values for alamethicin (see Scheme 1) calculated from amide hydrogen exchange protection factors in methanol (●), with values calculated from percentage hydrogen bond lifetimes from dynamics simulation with α-helical starting structure, using distance criteria of 2.5 (○), 2.7 (□), or 3.0 Å (△). Dotted lines are drawn to guide the eye.

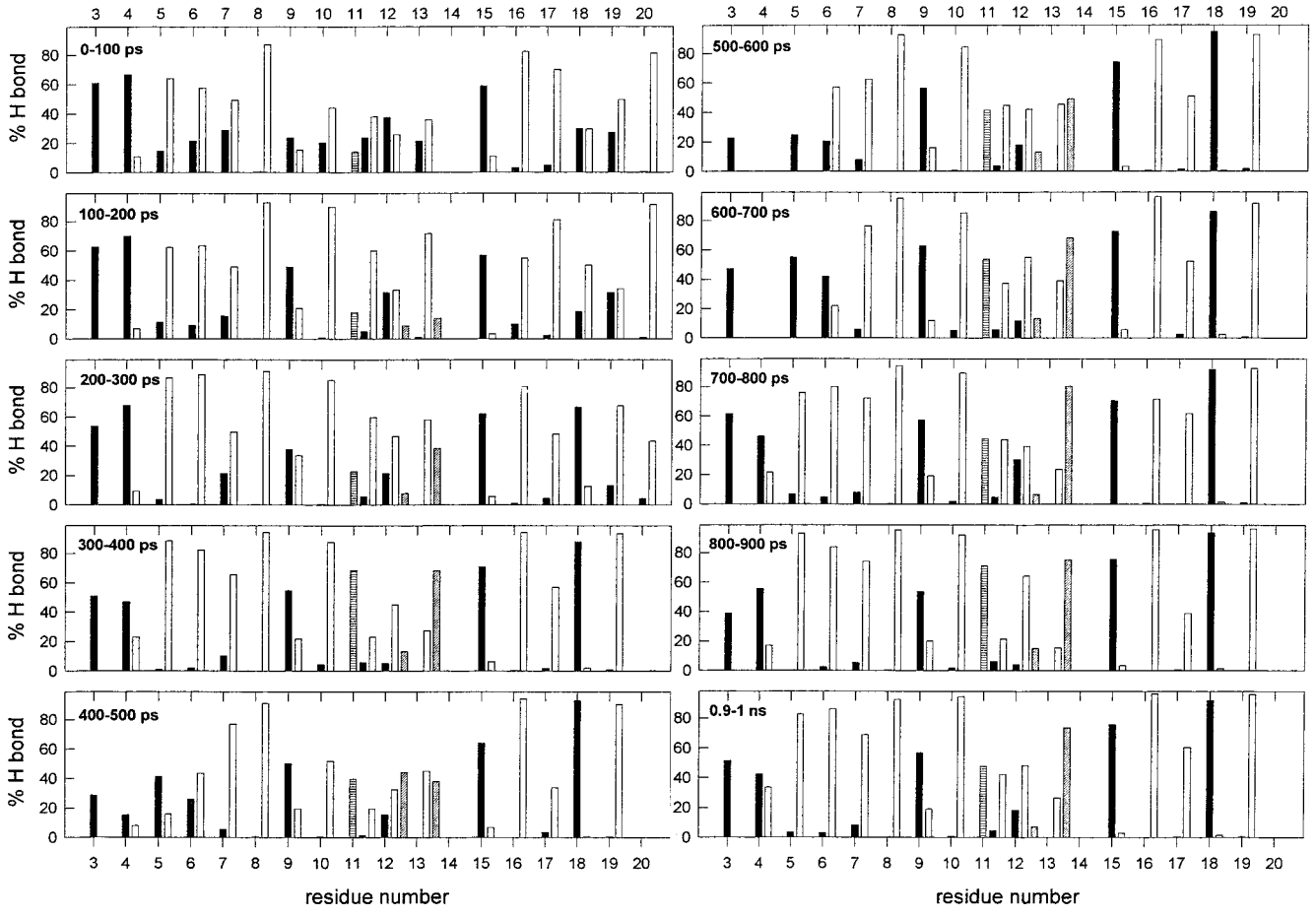

FIGURE 13 Percentage hydrogen bond lifetimes (3 Å criterion) for amide NH's of alamethicin averaged over 100-ps intervals of dynamics trajectories for the simulation from α-helical starting structure. Hydrogen bond types are designated by: γ-turn (G11 NH; *horizontal hash*), 3_{10} helix (*filled bars*), α-helix (*open bars*), and π-helix (*diagonal hash*). Space is allocated to γ- and π-hydrogen bonds only for residues 11–13, since the occurrence of these hydrogen bond types is negligible in other residues.

interactions between the extra α-methyl group on Aib_i with the β side chain atoms of residue $i + 3$ destabilize α-helical structure and promote 3_{10} helix (Marshall et al., 1990; Zhang and Hermans, 1994). Several such side chain interactions can be identified in the alamethicin α-helical starting structure (not shown), but these do not induce complete transition of α-helical hydrogen bonding to 3_{10} helix. While recent studies with spin-labeled peptides has suggested that 3_{10}-helical conformations may make a greater contribution to the structures of isolated helical polypeptides than previously thought (Fiori and Millhauser, 1995), alamethicin (and melittin) retains a largely α-helical conformation throughout the simulations. If the dominant polypeptide helical structure was 3_{10} helix, its extent should be maximized in peptides in nonaqueous solution (like methanol) where the extra intramolecular helical hydrogen bond is favored. Previous simulations have shown that conversion of polyAib α-helix to 3_{10} helix occurs on the 10–200-ps timescale in 10–14 residue peptides (Tirado-Rives et al., 1993; Zhang and Hermans, 1994); conversion of alamethicin to complete 3_{10} helix would be expected to occur during the 1-ns simulations if this was the energetically favorable conformation. Despite fluctuations that result in high levels of 3_{10} hydrogen bonds for residues 3–6 between 600 and 700 ps, for example (Fig. 13), the dominant 3_{10} hydrogen bonding patterns remain strictly local within a largely α-helical structure. These observations are in general agreement with the crystallographic studies, reviewed by Karle and Balaram (1990), on the effect of helix length and Aib content on the distribution of α and 3_{10} hydrogen bonds in Aib-containing helical polypeptides.

Effects of proline 14

The G11-P14 sequence of alamethicin and the G12-P14 sequence in melittin each display conformational diversity with associated variation in local hydrogen bonding. In addition to the effect of Pro (at residue *i*) in helical structure in promoting helix bending and 3_{10} hydrogen bonding involving the NH of residue $i + 1$ and the carbonyl of residue $i - 2$ (Piela et al., 1987; Fraternali, 1990; Yun et al., 1991; Sankararamakrishnan and Vishveshwara, 1993), there are two other similarities in the hydrogen bonding patterns of

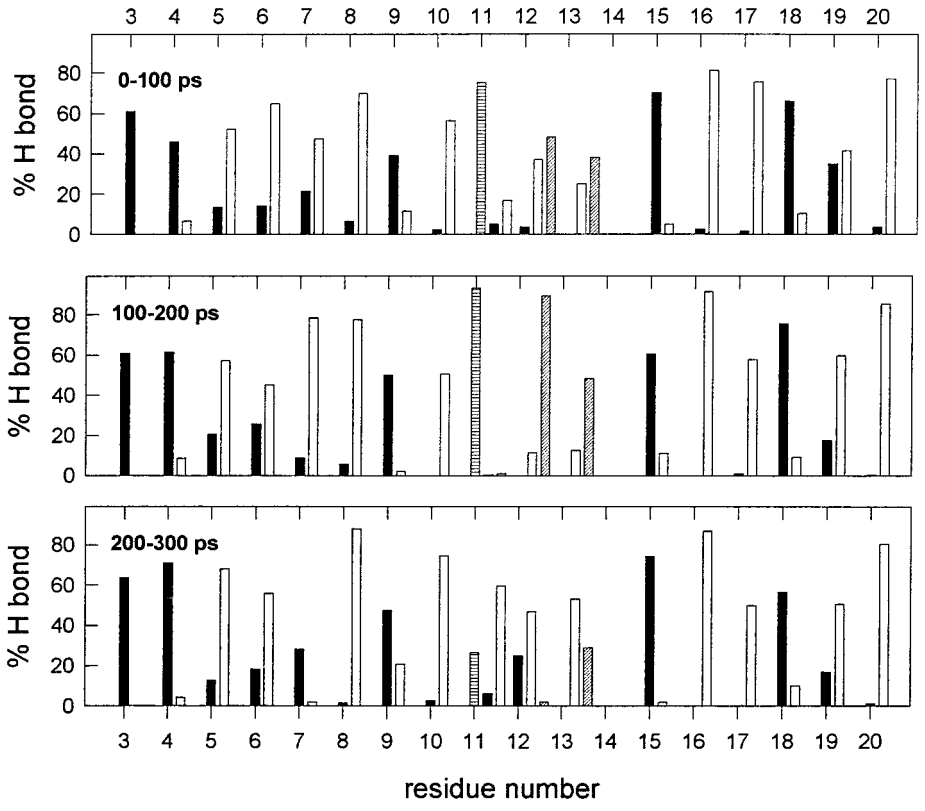

FIGURE 14 Percentage hydrogen bond lifetimes (3 Å criterion) for amide NH's of alamethicin averaged over 100-ps intervals of dynamics trajectories for the simulation from x-ray starting structure (first 300 ps only). Hydrogen bond types are designated by: γ-turn (G11 NH; *horizontal hash*), 3_{10} helix (*filled bars*), α-helix (*open bars*), and π-helix (*diagonal hash*). As in Fig. 13, space is allocated to γ- and π-hydrogen bonds only for residues 11–13.

melittin and alamethicin in this region, involving the formation of γ- and π-type hydrogen bonds. As described recently (Gibbs et al., 1997), the loss of hydrogen bond constraints on the carbonyl of Aib10 in alamethicin, together with the absence of β-atoms on Gly, allows the Aib10-Gly-11 peptide bond to partially reverse. In this state, the amide carbonyl projects away from the helix axis and the Gly NH forms an inverse γ-turn with good hydrogen bond geometry. A similar conformational transition involving the T11-G12 peptide bond is observed in the melittin simulations with the formation of a γ-turn stabilized by a G12 NH-T10 carbonyl peptide bond (Fig. 7). Reversible "flipping" of the X-Gly peptide bond may have a role in orienting the amide carbonyl for solvating the channel lumen, or providing additional cation binding sites (Sansom, 1992), in ion channel states of these peptides. The motif -G-X-X-P- (alamethicin) and -G-X-P- (melittin) is found in predicted transmembrane helices of several membrane ion channel proteins (unpublished observation), and similar peptide bond reversals with reorientation of the peptide carbonyl could have functional consequences.

The presence of glycine 2 or 3 residues before proline additionally deconstrains α-helical structure so that residues G12 and L13 (melittin) or G11, L12, and Aib13 (alamethicin) undergo transitions between different hydrogen bond patterns in which π-hydrogen bonds are abundant (Figs. 6, 13, and 14). In melittin, the π-helix may be associated with sequential loss of stable hydrogen bonding for residues 12 and 13 (Fig. 6) whereas in alamethicin, the interconversions of γ-turn and 3_{10}-, α-, and π-hydrogen bonding are maintained throughout the α-helical simulation (Fig. 13), so that overall levels of intramolecular hydrogen bonding remains high for these residues (Fig. 11). The "nonregular" hydrogen bonds allow the helical segments N- and C-terminal to P14 to bend away from each other while intramolecular hydrogen bonds are maintained (Gibbs et al., 1997), an observation which may explain the apparent incompatibility between high exchange stabilities of G11, L12, and Aib13 NH's in alamethicin (Dempsey, 1995; Fig. 12) and the evidence for helix bending from spin-relaxation experiments (North et al., 1995). Spyracopoulos et al. (1996) interpreted NMR relaxation parameters in terms of increased structural disorder around residues G11-L13 of alamethicin in methanol. This structural disorder, together with the overall decreased backbone order parameters in alamethicin compared with interior close-packed regions of proteins described by these authors, may result from local interconversion of intramolecular hydrogen bonding patterns as observed in the simulations.

Reliability of simulated structures

It may be questioned whether the dominant hydrogen bonding patterns observed in the simulations adequately represent the real situation. Several observations suggest that they do. The 3_{10} hydrogen bonds, highly populated for Aib3 and V15 of alamethicin, but not for A4 and A15 of melittin, are consistent with amide exchange stabilities. Secondly, both alamethicin simulations rapidly relax to the same hy-

drogen bond pattern which is recovered after large amplitude backbone fluctuations in which several hydrogen bonds are broken (see below). Since much of the deviation from regular α-helical structure results from the localized influence of side chains (e.g., the promotion of 3_{10} helix by Aib through steric effects), it is not surprising that the general structural features can be reproduced by dynamics simulations. These results are promising for the design and structure prediction of helical polypeptides, particularly those that interact with membranes and are soluble in nonaqueous solution where intramolecular hydrogen bonding is promoted. Previous experiments have shown that the "intrinsic" structural properties of these peptides, determined in methanol, are relevant for the membrane-reconstituted state (Dempsey et al., 1991; Dempsey and Butler, 1992; Dempsey and Handcock, 1996). The present study indicates that with correctly chosen initial conditions, including counterions and solvent composition, the intrinsic conformational properties of isolated helical peptides may be determined with an accuracy comparable with that obtained from routine NMR structural analysis. This conclusion is supported by recent successful comparisons of dynamics simulations of helical peptides with experimental measures of backbone conformations (e.g., Tirado-Rives et al., 1993; Zhang and Hermans, 1994), solvent effects (e.g., Kovacs et al., 1995), and hydrogen bond patterns and stabilities (Hirst and Brooks, 1995; Shirley and Brooks, 1997; see also Tobias et al., 1995).

The conformational properties of less-constrained regions are less easily confirmed since these are difficult to characterize experimentally; this is particularly so for structure near P14 in each peptide. In general, the experimental observation that intramolecular hydrogen bonds are maintained for amides of residues G11, L12, Aib13, and V15 of alamethicin (Dempsey, 1995) but not for G12, L13, and A15 of melittin (Dempsey, 1988; 1992) can be understood in relation to the persistent interconversion of intramolecular hydrogen-bonded structures for NH's of residues around P14 in alamethicin (Fig. 13) and the loss of stable hydrogen bonding for the corresponding residues in melittin (Fig. 6).

Since the melittin simulation underwent some progressive changes in hydrogen bonding at the N-terminus, and in the sequence before P14 (Fig. 6), it is not clear whether averaging of properties over the full simulation is a better description of the true conformational properties than an average over later periods of the simulation. Amide vicinal coupling constants calculated by averaging over the full simulation are closer to experimental values than those calculated from the final 200 ps of the simulation (Table 1). If this is taken to indicate that the behavior over the full simulation is a more accurate representation of the conformational properties in solution, then the partial unfolding of the N-terminal residues and loss of helical structure near P14 should be considered at least partially reversible, an expectation that can be tested in longer simulations.

There is generally a good agreement between measured coupling constants and those calculated from the simulations, particularly for amides in stable regions of structure (residues 7–11 and 19–23 in melittin; residues 4–9 of alamethicin; Table 1). The simulated coupling constants for alamethicin are similar to those calculated from the x-ray structure (Fox and Richards, 1982), but are generally larger, since backbone fluctuations around a stable helical structure will tend to increase the coupling constant. The main lack of agreement is in the C-terminal tripeptide sequence where the coupling constants from simulations are much larger than those calculated from the x-ray structure or measured in methanol (Table 1). This difference is probably due to the presence of E18 in the alamethicin variant used in the x-ray and solution NMR studies, since there is a much closer agreement between the simulated data and the measured coupling constants for Q18 alamethicin in detergent micelles (Table 1; Franklin et al., 1994).

Hydrogen bond opening and amide hydrogen exchange

Since fluctuations involving transient hydrogen bond "openings" are required for hydrogen exchange from hydrogen-bonded amides (Englander and Kallenbach, 1984), such fluctuations observed during the dynamics trajectories might provide pathways for exchange. Unfortunately, little is known about the amplitudes and timescales of these fluctuations, which are preequilibrium events preceding chemical exchange ($k_2 \gg k_3$ in Scheme 1; EX2 kinetics). The maintenance of EX2 kinetics at high pH for exchange from solvent-accessible helical amides in apamin (Dempsey, 1986) indicates, in that case, that the backbone fluctuations (strictly the closing rate constant, k_2) are faster than 0.1 ms. Although fluctuations underlying amide exchange from isolated helices probably occur on a faster timescale, there is no evidence that they occur on the nanosecond timescale accessible to simulation. The fluctuations underlying amide exchange may therefore be inadequately represented in the simulations. However, several conclusions can be made about the nature of the fluctuations that underlie amide exchange from these peptides in methanol.

First, despite indicating stable hydrogen-bonded structure, the simulated percentage hydrogen bond lifetimes, expressed as apparent equilibrium constants for hydrogen bond closing relative to opening, are considerably smaller than the experimental lifetimes calculated from amide exchange protection factors (Figs. 5 and 12). This has two contributions. First, low exchange protection factors ($<\sim$2-fold) cannot easily be measured, and amides that are not hydrogen-bonded (e.g., amides of residues 2 and 3 in melittin; Fig. 5), can have significant exchange protection, possibly resulting from steric hindrance to the formation of exchange intermediates. A second contribution results from the definition of hydrogen bond criteria in the simulations, which, in the most relaxed form, requires a hydrogen bond distance (NH—O) of $<$3 Å and an angle (N—H—O) $>$120°. As the hydrogen bond criterion is relaxed, the

TABLE 1 Simulated and experimental $^3J_{NHCH\alpha}$ coupling constants for alamethicin and melittin

		Esposito[#]							
Alamethicin	sim*	pH 9.1	pH 6.1	Franklin[§]	X-ray[¶]	Melittin	sim (0.5 ns)[‖]	sim (>0.3 ns)[‖]	Bazzo**
U1	(3.3)				2.7	G1	7.2	6.9	—
P2	(4.6)				3.4	I2	8.1	8.3	4.1
U3	(3.8)				3.4	G3	4.8	4.8	5.2/5.8
A4	5.7	5.6	5.5	4.8	4.3	A4	5.2	6.4	4.3
U5	(3.4)				3.1	V5	4.3	4.8	5.5
A6	5.9	4.7	4.9	5.0	5.6	L6	4.6	4.4	4.0
Q7	4.9	5.2	5.3	4.9	3.9	K7	5.0	5.1	4.5
U8	(3.4)				3.2	V8	5.1	4.8	5.1
V9	6.4	5.6	5.4	6.7	5.1	L9	4.8	4.5	4.8
U10	(4.2)				3.2	T10	6.6	6.9	6.6
G11	6.0	5.1/6.2	4.6/6.1	4.0/5.2	6.0	T11	6.3	8.2	6.3
L12	6.9	7.7	7.9	8.4	6.3	G12	4.6	2.6	5.5/5.5
U13	(3.0)				3.0	L13	4.4	4.4	3.7
P14	(5.0)				3.4	P14	—	—	—
V15	6.7	7.3	8.0	6.3	3.4	A15	7.5	7.5	5.3
U16	(3.4)				3.3	L16	4.3	4.4	5.0
U17	(3.7)				3.5	I17	4.2	4.0	4.6
Q18	8.0	5.3 (E18)	5.7 (E18)	7.5	5.1	S18	4.2	4.2	3.0
Q19	8.0	7.1	7.3	8.1	6.5	W19	4.6	4.6	4.5
Phol20	7.5	9.2	9.3	9.5	9.6	I20	4.3	4.3	4.4
						K21	4.3	4.1	4.1
						R22	4.9	5.1	4.7
						K23	4.3	4.3	4.7
						R24	5.9	5.7	4.9
						Q25	8.6	8.8	6.1
						Q26	7.2	7.0	7.4

*Coupling constants ($^3J_{NHCH\alpha}$) calculated from molecular dynamics simulation as described in the text. Values in brackets are apparent coupling constants for residues lacking an α-proton (Aib) or NH (Pro).

[#]Measured coupling constants for E18-alamethicin in methanol (Esposito et al., 1987).

[§]Measured coupling constants for alamethicin in aqueous SDS micelles (Franklin et al., 1994).

[¶]Apparent coupling constants calculated from the structure of alamethicin (molecule A) crystallized from methanol (Fox and Richards, 1982).

[‖]Coupling constants ($^3J_{NHCH\alpha}$) calculated from molecular dynamics simulation of melittin in methanol with counter ions, averaged over the full trajectory, and the final 200 ps, respectively.

**Measured coupling constants for melittin in methanol (Bazzo et al., 1988).

simulated apparent hydrogen bond lifetimes increase (Figs. 5 and 12), and can be made to approach the experimental hydrogen bond lifetimes with an upper distance criterion of 3.5 to 4 Å (not shown). While this does not necessarily indicate that hydrogen bond breaking fluctuations involving NH—O separations of >3.5 or 4 Å are required for exchange, it does suggest that the rapid small amplitude fluctuations involving small (~1 Å) excursions from acceptable hydrogen bond geometry are not pathways for hydrogen exchange in these peptides. This doesn't exclude the possibility that such small amplitude fluctuations might underlie exchange from some interior sites in proteins where larger amplitude fluctuations are rarer (Englander and Kallenbach, 1984).

Secondly, while fluctuations involving cooperative "opening" of several sequential hydrogen bonds were not systematically analyzed, these might be important for amide exchange from isolated helices. In melittin, similar exchange protection factors among interior amides in the N-terminal helix and among those in the C-terminal helix indicated that these amides might exchange during concerted hydrogen bond opening fluctuations (Dempsey, 1988). Backbone fluctuations that separate the amide NH and carbonyl partners of a single hydrogen bond by >3.5–4 Å are not easily accommodated in isolated helices without disrupting adjacent hydrogen bonds, supporting the expectation that fluctuations involving concerted "opening" of several sequential hydrogen bonds are required for exchange of interior amides *in isolated helices*. Finally, comparison of protection factors for acid- and base-catalyzed exchange in a polyalanine-based helical peptide in water (Rohl and Baldwin, 1994) and alamethicin in methanol (Dempsey, 1995) indicates that cooperative fluctuations involving concerted freeing of the amide NH and carbonyl of the same peptide bond make at least some contribution to acid-catalyzed exchange.

Many large-amplitude fluctuations were observed in the simulations, illustrating both the general stability of hydrogen-bonded structure (through its recovery after conformational excursions) and potential fluctuational pathways for amide exchange. An example from the α-helical alamethicin simulation (Fig. 15) represents one of a number of fluctuations in which an internal turn of helix reversibly "opens" with concerted breaking of several hydrogen bonds

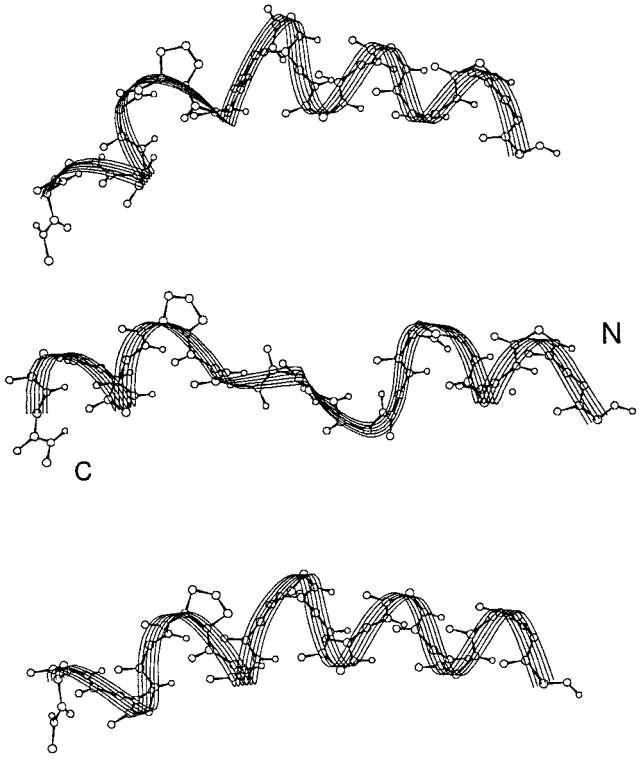

FIGURE 15 Backbone structure of alamethicin after 780, 800, and 820 ps (*top to bottom*) of dynamics simulation in methanol from α-helical starting structure showing reversible opening of a central helical region with loss and recovery of hydrogen bonds involving V9 to L12 NH's.

(involving V9 to L12 NH's in this case). In the "open" state the four amide NH's are splayed out from the helix axis and are presumable exchangeable. The lifetime of this "open" state (~40 ps), and of other "open" states involving reversible breaking of several hydrogen bonds (20–100 ps), may be sufficiently long for catalyzed exchange to occur. Since these fluctuations are poorly represented within the 1-ns simulation, a quantitative analysis of their contribution to amide exchange in comparison with experimental exchange protection factors cannot be made at this stage. However, longer dynamics simulations may reveal whether such large-amplitude fluctuations provide better quantitative comparisons with experimental protection factors. Since the helical hydrogen-bonded structures of the peptides are stable during dynamics simulation in methanol, the solvated systems described here are promising candidates for extended simulations.

We are grateful to Dr. Phil Williams for assistance with the simulations.

This work was supported by grants from the Biotechnology and Biological Sciences Research Council (GR/H36443), the Nuffield Foundation (SCI/180/91//46G), and the Wellcome Trust (040106/Z/93); the BBSRC also supports the Bristol Centre for Molecular Recognition.

REFERENCES

Bai, Y., J. S. Milne, L. Mayne, and S. W. Englander. 1993. Primary structure effects on peptide group hydrogen exchange. *Proteins Struct. Funct. Genet.* 17:75–86.

Baker, E. N., and R. E. Hubbard. 1984. Hydrogen-bonding in globular-proteins. *Prog. Biophys. Molec. Biol.* 44:97–179.

Barranger-Mathys, M., and D. S. Cafiso. 1996. Membrane structure of voltage-gated channel-forming peptides by site-directed spin-labeling. *Biochemistry*. 35:498–505.

Bazzo, R., M. J. Tappin, A. Pastore, T. S. Harvey, J. A. Carver, and I. D. Campbell. 1988. The structure of melittin in solution. *Eur. J. Biochem.* 173:139–146.

Dauber-Osguthorpe, P., V. A. Roberts, D. J. Osguthorpe, J. Wolff, M. Genest, and A. T. Hagler. 1988. Structure and energetics of ligand-binding to proteins—*Escherichia-coli* dihydrofolate reductase trimethoprim, a drug-receptor system. *Proteins Struct. Funct. Genet.* 4: 31–47.

Dempsey, C. E. 1986. pH-Dependence of hydrogen exchange from backbone peptide amides of apamin. *Biochemistry.* 25:3904–3911.

Dempsey, C. E. 1988. pH-Dependence of hydrogen exchange from backbone peptide amides of melittin in methanol. *Biochemistry.* 27: 6893–6901.

Dempsey, C. E. 1992. Quantitation of the effects of an internal proline residue on individual hydrogen bond stabilities in an isolated helix: pH-dependent amide exchange in melittin and [Ala-14]melittin. *Biochemistry.* 31:4705–4712.

Dempsey, C. E. 1995. Hydrogen bond stabilities in the isolated alamethicin helix: pH-dependent amide exchange measurements in methanol. *J. Am. Chem. Soc.* 117:7526–7534.

Dempsey, C. E., R. Bazzo, T. S. Harvey, I. Syperek, G. Boheim, and I. D. Campbell. 1991. Contribution of proline-14 to the structure and actions of melittin. *FEBS Lett.* 281:240–244.

Dempsey, C. E., and G. S. Butler. 1992. Hydrogen bond stabilities in membrane-reconstituted melittin from amide-resolved, hydrogen exchange measurements. *Biochemistry.* 31:11973–11977.

Dempsey, C. E., and L. J. Handcock. 1996. Hydrogen bond stabilities in membrane-reconstituted alamethicin from amide-resolved hydrogen-exchange measurements. *Biophys. J.* 70:1777–1788.

Duclohier, H., G. Molle, J. Y. Dugast, and G. Spach. 1992. Prolines are not essential residues in the barrel-stave model for ion channels induced by alamethicin analogs. *Biophys. J.* 63:868–873.

Englander, S. W., and N. S. Kallenbach. 1984. Hydrogen exchange in proteins. *Q. Rev. Biophys.* 16:521–655.

Esposito, G., J. A. Carver, J. Boyd, and I. D. Campbell. 1987. High resolution ^{1}H NMR study of the solution structure of alamethicin. *Biochemistry.* 26:1043–1050.

Fiori, W. R., and G. L. Millhauser. 1995. Exploring the peptide 3_{10}-α helix equilibrium with double label electron spin resonance. *Biopolymers*. 37:243–250.

Fox, R. O., and F. M. Richards. 1982. A voltage-gated ion channel model inferred from the crystal structure of alamethicin at 1.5 Å resolution. *Nature*. 300:325–330.

Franklin, J. C., J. F. Ellena, S. Jayasinghe, L. P. Kelsh, and D. S. Cafiso. 1994. Structure of micelle-associated alamethicin from ^{1}H NMR—evidence for conformational heterogeneity in a voltage-gated peptide. *Biochemistry.* 33:4036–4045.

Fraternali, F. 1990. Restrained and unrestrained molecular dynamics simulations in the NVT ensemble of alamethicin. *Biopolymers*. 30: 1083–1099.

Gibbs, N., R. B. Sessions, P. B. Williams, and C. E. Dempsey. 1997. Helix bending in alamethicin: molecular dynamics simulations and amide hydrogen exchange in methanol. *Biophys. J.* 72:2490–2495.

Hirst, J. D., and C. L. Brooks. 1995. Molecular dynamics simulations of isolated helices of myoglobin. *Biochemistry.* 34:7614–7621.

Hvidt, A., and S. O. Neilsen. 1966. Hydrogen bonding in proteins. *Adv. Protein Chem.* 21:287–386.

Karle, I., and P. Balaram. 1990. Structural characteristics of α-helical peptide molecules containing Aib residues. *Biochemistry*. 29: 6747–6756.

Kitao, A., F. Hirata, and N. Go. 1993. Effects of solvent on the conformation and the collective motions of a protein. 2. Structure of hydration in melittin. *J. Phys. Chem.* 97:10223–10230.

Kitson, D. H., F. Avbelj, J. Moult, D. T. Nguyen, J. E. Mertz, D. Hadzi, and A. T. Hagler. 1993. On achieving better than 1-angstrom accuracy in a

simulation of a large protein. Streptomyces-griseus protease A. *Proc. Natl. Acad. Sci. U.S.A.* 90:8920–8924.

Kovacs, H., A. E. Mark, J. Johansson, and W. F. VanGunsteren. 1995. The effect of environment on the stability of an integral membrane helix—molecular dynamics simulations of surfactant protein-c in chloroform, methanol and water. *J. Mol. Biol.* 247:808–822.

Marshall, G. R., E. E. Hodgkin, G. Langs, D. Smith, J. Zabrocki, and M. T. Leplawy. 1990. Factors governing helical preference of peptides containing multiple α,α-dialkyl amino-acids. *Proc. Natl. Acad. Sci. U.S.A.* 87:487–491.

North, C. L., J. C. Franklin, R. G. Bryant, and D. S. Cafiso. 1994. Molecular flexibility demonstrated by paramagnetic enhancements of nuclear-relaxation: application to alamethicin, a voltage-gated peptide channel. *Biophys. J.* 67:1861–1866.

Osguthorpe, D. J., and P. Dauber-Osguthorpe. 1992. FOCUS—a program for analyzing molecular-dynamics simulations featuring digital signal-processing techniques. *J. Mol. Graphics*. 10:178–184.

Pardi, A., M. Billeter, and K. Wuthrich. 1984. Calibration of the angular-dependence of the amide proton-Cα proton coupling constants, ^{3}JNHα, in a globular protein-use of ^{3}JNHα for identification of helical structure. *J. Mol. Biol.* 180:741–745.

Pastore, A., T. S. Harvey, C. E. Dempsey, and I. D. Campbell. 1989. The dynamic properties of melittin in solution. *Eur. Biophys. J.* 16:363–367.

Piela, L., G. Nemethy, and H. Scheraga. 1987. Proline-induced constraints in α-helices. *Biopolymers*. 26:1587–1600.

Rohl, C. A., and R. A. Baldwin. 1994. Exchange kinetics of individual amide protons in 15-N labeled helical peptides measured by isotope-edited NMR. *Biochemistry.* 33:7760–7767.

Rose, G. D., L. M. Gierasch, and J. A. Smith. 1985. Turns in peptides and proteins. *Adv. Protein Chem.* 37:1–109.

Sankararamakrishnan, R., and S. Vishveshwara. 1993. Characterization of proline-containing α-helix (helix F model of bacteriorhodopsin) by molecular dynamics studies. *Proteins Struct. Funct. Genet.* 15:26–41.

Sansom, M. S. P. 1992. Proline residues in transmembrane helices of channel and transport proteins: a molecular modelling study. *Protein Eng.* 5:53–60.

Sansom, M. S. P. 1993. Structure and function of channel-forming peptaibols. *Q. Rev. Biophys.* 26:365–421.

Schiffer, C. A., and W. F. VanGunsteren. 1996. Structural stability of disulfide mutants of basic pancreatic trypsin inhibitor—a molecular dynamics study. *Proteins Struct. Funct. Genet.* 26:66–71.

Sessions, R. B., P. Dauber-Osguthorpe, and D. J. Osguthorpe. 1989. Filtering molecular-dynamics trajectories to reveal low-frequency collective motions: phospholipase-A_2. *J. Mol. Biol.* 210:617–633.

Shirley, W. A., and C. L. Brooks. 1997. Curious structures in "canonical" alanine-based peptides. *Proteins.* 28:59–71.

Spyracopoulos, L., A. A. Yee, and J. D. J. O'Neil. 1996. Backbone dynamics of an alamethicin in methanol and aqueous detergent solution determined by heteronuclear ^{1}H-^{15}N NMR spectroscopy. *J. Biomol. NMR.* 7:283–294.

Tauer, K. J., and W. Lipscomb. 1952. The crystal structure, residual entropy and dielectric anomaly of methanol. *Acta Crystallogr.* 5:606–612.

Terwilliger, T. C., and D. Eisenberg. 1982. The structure of melittin. Interpretation of the structure. *J. Biol. Chem.* 257:6016–6022.

Tirado-Rives, J., D. S. Maxwell, and W. L. Jorgensen. 1993. Molecular dynamics and Monte Carlo simulations favor the α-helical form for alanine-based peptides in water. *J. Am. Chem. Soc.* 115:11590–11593.

Tobias, D. J., J. Gesell, M. L. Klein, and S. J. Opella. 1995. A simple protocol for identification of helical and mobile residues in membrane proteins. *J. Mol. Biol.* 253:391–395.

Weast, R. C. 1976. Handbook of Chemistry and Physics, Vol. 57. CRC Press, Cleveland. E-64.

Yee, A. A., R. Babiuk, and J. D. J. O' Neil. 1995. The conformation of an alamethicin in methanol by multinuclear NMR-spectroscopy and distance geometry simulated annealing. *Biopolymers*. 36:781–792.

Yee, A. A., and J. D. J. O'Neil. 1992. Uniform ^{15}N labeling of a fungal peptide: the structure and dynamics of alamethicin by ^{15}N and ^{1}H NMR spectroscopy. *Biochemistry.* 31:3135–3143.

Young, M. A., B. Jayaram, and D. L. Beveridge. 1997. Intrusion of counterions into the spine of hydration in the minor groove of B-DNA: fractional occupancy of electronegative pockets. *J. Am. Chem. Soc.* 119:59–69.

Yun, R. H., A. Anderson, and J. Hermans. 1991. Proline in α-helix: stability and conformation studied by dynamics simulation. *Proteins Struct. Funct. Genet.* 10:219–228.

Zhang, L., and J. Hermans. 1994. 3_{10} Helix versus α-helix: a molecular dynamics study of conformational preferences of Aib and alanine. *J. Am. Chem. Soc*. 116:11915–11921.